2020 IEEE International Conference on Robotics and Automation (ICRA)
31 May - 31 August, 2020. Paris, France

# Time Optimal Motion Planning with ZMP Stability Constraint for Timber Manipulation

Jiazhi Song[1] and Inna Sharf[2]

*Abstract*— **This paper presents a dynamic stability-constrained optimal motion planning algorithm developed for a timber harvesting machine working on rough terrain. First, the kinematics model of the machine, and the Zero Moment Point (ZMP) stability measure is presented. Then, an approach to simplify the model to gain insight and achieve a fast solution of the optimization problem is introduced. The performance and computation time of the motion plan obtained with the simplified model is compared against that obtained with the full kinematics model of the machine with the help of MATLAB simulations. The results demonstrate feasibility of fast motion planning while satisfying the dynamic stability constraint.**

## I. Introduction

Timber harvesting is a very important industry for many countries including Canada. The majority of modern timber harvesting businesses worldwide employ feller-bunchers and timber harvesters to fell trees, and use skidders and forwarders to transport felled trees for further processing. The aforementioned machines can be considered as a type of mobile manipulator since they consist of mobile bases and hydraulically powered mechanized arms with multiple degrees of freedom. Nowadays, the machines still fully rely on operator judgement and control in order to function [1]. The lack of machine automation in the timber harvesting industry results in high operator training costs and suboptimal efficiency in harvesting; there is a strong impetus for developing an autonomous harvesting system.

Some progress has been made to increase the timber harvesting machines' autonomy. The dynamics model of a timber harvester is presented in [2]; the teleoperation of a forestry manipulator is showcased in [3]; the hydraulic actuator control of a forwarder machine has been discussed in [4] [5], and the motion control of a forestry manipulator along a fixed path is presented in [6]. However, a versatile motion planning algorithm that is tailored to the specific challenges of timber harvesting is yet to be developed.

The prevention of roll-over is of great importance in this application as rolling over poses a lot of risks. Timber harvesting machines are prone to roll over as they have a high center of mass, manipulate heavy trees, and inevitably have to operate on slopes and in adverse weather conditions. There is a variety of results on manipulator and mobile manipulator optimal motion planning [7]–[10] but none of the previous works address the problem of roll-over prevention.

Some measures that were designed to quantify the proximity to a roll-over condition through force and moment measurement include the method introduced in [11], the force-angle stability measure in [12]–[14], and the lateral load transfer (LLT) parameter [15]–[17]. However, the measures require force measurements at joints or wheels and cannot provide any guidelines for motion planning. Considering the complex structure of humanoid robots and the effect of momentum caused by different motions, the zero moment point (ZMP) stability measure was introduced in [18]. Even though the ZMP measure can be too conservative in a walking robot scenario, it is appropriate for a timber harvesting machine since the base of the machine normally maintains full contact with the ground.

The ZMP properties of mobile manipulators are considered in [19] but it is assumed that the robot base is situated on a horizontal plane and motion planning was not addressed. In [20], ZMP measure is used as a constraint in the model predictive control formulation for the path following of a forklift. Dynamically stable motion planning methods based on ZMP compensation for mobile manipulators also exist in the literature. ZMP compensating motions are created by the mobile base in [21] and [22], while they are obtained through moving the manipulator arm as directed by a potential function in [23]–[25]. However, none of the aforementioned works consider optimal dynamically stable motion planning for manipulation. Furthermore, considering the requirement for efficient machine operation, we are interested in fast optimal planning solutions that could allow for near real-time guidance of the machine during operation.

In this paper, a feller buncher machine is considered as the example of timber harvesting machines. In Section II, the kinematics model of the machine and the ZMP measure formulation are introduced as the theoretical background. In Section III, the optimal control formulation of the motion planning problem is presented subject to the ZMP stability constraint. In light of the high dimensionality of the full model and the resulting computational complexity of solving the optimal motion planning problem, we propose a simplified model of the feller buncher; this model also allows us to obtain analytical solution to the motion planning problem under certain assumptions. Simulation results showcasing the motion plan will be presented in Section IV. Discussion and potential future work will be mentioned in Section V.

Both authors are with department of Mechanical Engineering, McGill University, Montreal, QC H3A 0C3, Canada [1]jiazhi.song@mail.mcgill.ca [2]inna.sharf@mcgill.ca

## II. Theoretical Background

### A. Kinematics of Feller Buncher Machine

In order to accommodate the constraints imposed by the machine's joint properties and ZMP stability, we first derive the full kinematic model of the feller buncher. The manipulator arm of the machine has 5 joint DoFs, and the tracked base is modeled as a unicycle on arbitrary terrain. To better illustrate the kinematics derivation, the schematic of a feller buncher with an articulated arm is shown in Figure 1.

Frame $\mathcal{O}$ is the inertial frame, and frame $\mathcal{F}_i$ is fixed to the $i$-th link of the machine for $i \in \{0, 1, 2, 3, 4, 5\}$. Here, link 0 refers to the machine's undercarriage, and frame $\mathcal{F}_0$ is fixed on the undercarriage at $\boldsymbol{p}_b$. Link 1 refers to the cabin and engine component, links 2 to 4 refer to the arm components, and link 5 refers to the machine's end effector. The three axes of each link frame $\boldsymbol{x}_i$, $\boldsymbol{y}_i$, and $\boldsymbol{z}_i$ are represented by red, green, and blue arrows, respectively. The axis of rotation for each link is: $\boldsymbol{z}_1$ for link 1, $\boldsymbol{x}_2$ for link 2, $\boldsymbol{x}_3$ for link 3, $\boldsymbol{x}_4$ for link 4, and $\boldsymbol{z}_5$ for link 5.

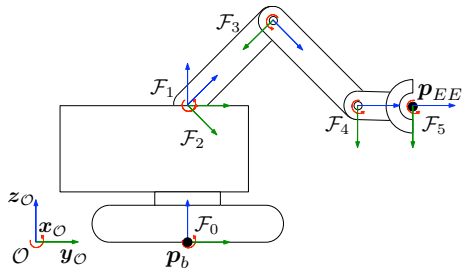


Fig. 1: Schematic diagram of a feller buncher with an articulated arm.

We denote the angle of joint $i$ between link $i$ and $i-1$ with $q_i \in \mathbb{R}$ $(i = 1, \ldots, 5)$, and collect all joint angles into a column vector $\boldsymbol{q} = [q_1, q_2, q_3, q_4, q_5]^T$, and consider the undercarriage-fixed frame $\mathcal{F}_0$ to undergo a $\boldsymbol{z}$-$\boldsymbol{x}$-$\boldsymbol{y}$ rotation from initial attitude with each angle represented by $\psi$ (yaw), $\theta$ (pitch), and $\phi$ (roll). The Cartesian coordinates of each component's center of mass relative to $\boldsymbol{p}_b$ expressed in $\mathcal{F}_0$, $\boldsymbol{p}_i^{\mathcal{F}_0}$, can be found similarly and written succinctly by introducing $\bar{\boldsymbol{q}} = [\boldsymbol{p}_b^{\mathcal{O}^T}, \psi, \theta, \phi, \boldsymbol{q}^T]^T$ as:

$$\boldsymbol{p}_i^{\mathcal{F}_0} = \boldsymbol{f}_i(\bar{\boldsymbol{q}}). \tag{1}$$

From (1), we also obtain the inertial accelerations of links' centers of mass expressed in $\mathcal{F}_0$, which will be needed for the dynamics analysis later:

$$\begin{aligned} \dot{\boldsymbol{p}}_i^{\mathcal{F}_0} &= \boldsymbol{J}_{pi}(\bar{\boldsymbol{q}})\dot{\bar{\boldsymbol{q}}}, \\ \ddot{\boldsymbol{p}}_i^{\mathcal{F}_0} &= \dot{\boldsymbol{J}}_{pi}(\bar{\boldsymbol{q}})\dot{\bar{\boldsymbol{q}}} + \boldsymbol{J}_{pi}(\bar{\boldsymbol{q}})\ddot{\bar{\boldsymbol{q}}}, \end{aligned} \tag{2}$$

where we introduced the position kinematics Jacobian, $\boldsymbol{J}_{pi}(\bar{\boldsymbol{q}}) = \frac{\partial \boldsymbol{f}_i}{\partial \bar{\boldsymbol{q}}}$. We can also write out the inertial angular velocity and angular acceleration of the $i$-th component expressed in $\mathcal{F}_i$, $\boldsymbol{\omega}_i^{\mathcal{F}_i}$ and $\dot{\boldsymbol{\omega}}_i^{\mathcal{F}_i}$ as

$$\begin{aligned} \boldsymbol{\omega}_i^{\mathcal{F}_i} &= \boldsymbol{J}_{\omega i}(\bar{\boldsymbol{q}})\dot{\bar{\boldsymbol{q}}}, \\ \dot{\boldsymbol{\omega}}_i^{\mathcal{F}_i} &= \dot{\boldsymbol{J}}_{\omega i}(\bar{\boldsymbol{q}})\dot{\bar{\boldsymbol{q}}} + \boldsymbol{J}_{\omega i}(\bar{\boldsymbol{q}})\ddot{\bar{\boldsymbol{q}}}. \end{aligned} \tag{3}$$

As noted earlier, we consider the tracked base as a unicycle model and the feller buncher is therefore subject to control input $\boldsymbol{u} = [u_a, u_\psi, \boldsymbol{u}_q^T]^T$, where $u_a$, $u_\psi$, and $\boldsymbol{u}_q$ represent acceleration along heading direction, yaw angular acceleration, and manipulator arm joint accelerations, respectively. Defining $\boldsymbol{x} = [\bar{\boldsymbol{q}}^T, \dot{\bar{\boldsymbol{q}}}^T]^T$, the feller buncher's kinematics equation can be written as:

$$\dot{\boldsymbol{x}} = g(\boldsymbol{x}, \boldsymbol{u}). \tag{4}$$

Eq. (4) serves as the model of the machine for the optimal motion planning problem.

### B. Dynamic Stability of Feller Buncher Machine

Since the ZMP measure is capable of quantifying the stability margin of a mobile manipulator using only kinematics information and inertia parameters instead of a full dynamics model of the machine or force measurements, it becomes our method of choice due to the potential benefit of faster motion planning calculations and its practicality.

According to [19], letting $\boldsymbol{p}_i^{\mathcal{F}_0} = [x_i, y_i, z_i]^T$, $\ddot{\boldsymbol{p}}_i^{\mathcal{F}_0} = [\ddot{x}_i, \ddot{y}_i, \ddot{z}_i]^T$, and the gravitational vector $\boldsymbol{g}^{\mathcal{F}_0} = [g_x, g_y, g_z]^T$, the coordinates of ZMP location $\boldsymbol{p}_{zmp}^{\mathcal{F}_0} = [x_{zmp}, y_{zmp}, 0]^T$ are expressed as:

$$\begin{aligned} x_{\text{zmp}} &= \frac{\sum_i m_i(\ddot{z}_i - g_z)x_i - \sum_i m_i(\ddot{x}_i - g_x)z_i}{\sum_i m_i(\ddot{z}_i - g_z)} \\ y_{\text{zmp}} &= \frac{\sum_i m_i(\ddot{z}_i - g_z)y_i - \sum_i m_i(\ddot{y}_i - g_y)z_i}{\sum_i m_i(\ddot{z}_i - g_z)}. \end{aligned} \tag{5}$$

Note that differently from the formulations presented in previous works [19], the signs in front of the gravitational acceleration components are negative since gravity should be treated as an external force on the system. Mass of the tree is assumed to be known in this work. With $S$ representing the machine's support polygon, the machine is dynamically stable when $\boldsymbol{p}_{zmp} \in Conv(S)$, but has the tendency to rollover otherwise. Equation (5) can be evaluated by substituting from the kinematics equations (1), (2), and (3) represented in $\mathcal{F}_0$, once the joint motions have been planned, to produce the ZMP locus, i.e., the trajectory of ZMP in $\mathcal{F}_0$ during the motion of the machine.

## III. Simplified Model of Feller Buncher

Due to the high dimensionality of the kinematics model (4), the nonlinearity that resides in the forward kinematics equation (1) and the ZMP formulation (5), the solution of the optimal motion planning problem requires longer than practical computation time for real-time guidance, even for a case where the base does not move. In order to develop a real-time motion planner for the machine, a simplification of the machine is called upon.

To simplify the optimal control problem by reducing the dimension of the problem, and considering typical modes of operation of the feller buncher, the 5-joint-DoF manipulator

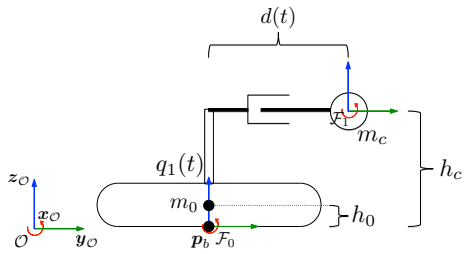


Fig. 2: Schematic diagram of a simplified feller buncher.

arm is approximated by a single lumped mass that rotates around the machine's cabin yaw axis (joint $q_1$) with a variable radius $d(t)$. The simplified model is illustrated schematically in Figure 2. The simplification is also based on the following assumptions:

**Assumption 1.** *a) The mobile base has a fixed attitude and performs prescribed acceleration along $\boldsymbol{y}_0$ direction. b) The end effector maintains the same attitude in $\mathcal{F}_1$ and moves within the $x$-$y$ plane of $\mathcal{F}_1$. c) The boom (link 2) and stick (link 3) are of the same length.*

Note that in practice, a feller buncher rarely moves its base while holding up a tree except when its immediate surroundings are occupied and it has to back up or move forward to place the tree down and therefore, Assumption 1a) can be justified for most cases. To mitigate the limitations caused by Assumption 1b), a specially designed motion planner can manipulate the end effector into or out of the $x$-$y$ plane of $\mathcal{F}_1$ without significant loss in performance as the vertical movements required are usually small. Assumption 1c) is proposed as it is the case with the specific feller buncher model this research is based on, and it makes analytical formulations easier to compute. However, the analytical and simulation results presented in the following sections can be easily generalized to the cases where Assumption 1 c) does not hold.

In the simplified model, the height of the lumped mass $m_c$, denoted as $h_c$, changes when the load being carried by the end effector changes. Since load changing only occurs at tree pick-up and drop-off, $h_0$ and $h_c$ can be treated as constants. The angle of joint 1, $q_1$, and the distance $d$ between the slew joint axis and lumped mass $m_c$, are the two joint DOFs of the simplified model. The control inputs of the simplified model are $u_{q_1}$, joint acceleration of $q_1$, and $u_d$, the second order derivative of $d$ with respect to time.

The kinematics model of the simplified model is straightforward to derive and can be written as well in the general form:

$$\dot{\tilde{\boldsymbol{x}}} = \tilde{g}(\tilde{\boldsymbol{x}}, \tilde{\boldsymbol{u}}), \tag{6}$$

where $\tilde{\boldsymbol{x}} = [q_1, \dot{q}_1, d, \dot{d}]^T$, and $\tilde{\boldsymbol{u}} = [u_{q_1}, u_d]$.

### A. Mapping from Simplified Model to Full Model

Since the simplified manipulator model has 2 DoFs while the full model has 5 DoFs, to ensure that the center of mass location of the full model follows that of $m_c$, a connection between the DoFs of the simplified model and those of the full model of the machine needs to be made. From Assumption 1 b) and c), the machine's joint angles are constrained such that

$$[q_3, q_4, q_5]^T = [-\pi - 2q_2, \frac{\pi}{2} + q_2, \text{constant}]^T, \tag{7}$$

and the corresponding relationship between joint accelerations follows:

$$[\ddot{q}_3, \ddot{q}_4, \ddot{q}_5]^T = [-2\ddot{q}_2, \ddot{q}_2, 0]^T. \tag{8}$$

Defining the constant distance between the $i$-th link's center of mass and its rotational axis as $r_i$, and the lengths of link 2 and link 4 as $l_2$ and $l_4$, respectively, the relationship between $d$ and $q_2$ can be written as:

$$d = \frac{m_1 r_1 + m_4 r_4 + m_5 l_4 - \Delta \sin q_2}{\sum_{i=1}^5 m_i}, \tag{9}$$

where $\Delta = m_2 r_2 + m_3 l_2 + m_3 r_3 + 2m_4 l_2 + 2m_5 l_2$. Then we get

$$q_2 = \sin^{-1}\left(\frac{m_1 r_1 + m_4 r_4 + m_5 l_4 - \sum_{i=1}^5 m_i d}{\Delta}\right). \tag{10}$$

By taking the first and second derivative of (9) with respect to time, we can obtain:

$$\begin{aligned} \dot{q}_2 &= \frac{-\sum_{i=1}^5 m_i \dot{d}}{\Delta \cos q_2} \\ \ddot{q}_2 &= \frac{\sum_{i=1}^5 m_i \ddot{d} - \Delta \sin q_2 \dot{q}_2^2}{-\Delta \cos q_2}. \end{aligned} \tag{11}$$

Therefore, using the mapping provided in (10) and (11), and the relation between joint angles and accelerations as given in (7) and (8), the ZMP location of the full kinematics model can be written as $\boldsymbol{p}_{zmp}(\tilde{\boldsymbol{x}}, \tilde{\boldsymbol{u}})$.

### B. Physical Interpretation

Further insights and physical interpretation of ZMP locus can be gathered by making the following additional assumptions on the model in Figure 2:

**Assumption 2.** *a) The machine remains on a horizontal surface, hence $g_x = g_y = 0$ and $g_z = -g$, where $g$ is the gravitational constant. b) The distance $d$ remains constant. c) The behavior of $\ddot{q}_1$ represents that of a step response, so $\dddot{q}_1 = 0$ almost everywhere. d) The $x$ and $y$ coordinates of the center of mass of the tracked base equal to 0 when expressed in $\mathcal{F}_0$.*

With the above assumptions, the center of mass position of $m_0$ with respect to $\boldsymbol{p}_b$ can then be expressed in $\mathcal{F}_0$ by

$$[x_0, y_0, z_0]^T = [0, 0, h_0]^T, \tag{12}$$

and the inertial acceleration of $m_0$ can be expressed in $\mathcal{F}_0$ as

$$[\ddot{x}_0, \ddot{y}_0, \ddot{z}_0]^T = [0, u_a, 0]^T. \tag{13}$$

The position of the point mass $m_c$ with respect to $\boldsymbol{p}_b$ is then given in $\mathcal{F}_0$ by

$$[x_c, y_c, z_c]^T = [-d\sin q_1, d\cos q_1, h_c]^T, \tag{14}$$

and inertial acceleration of $m_c$ expressed in $\mathcal{F}_0$:

$$\begin{aligned}
\ddot{x}_c &= -\ddot{d}\sin q_1 - 2\dot{d}\cos q_1\dot{q}_1 + d\sin q_1\dot{q}_1^2 - d\cos q_1\ddot{q}_1 \\
\ddot{y}_c &= \ddot{d}\cos q_1 - 2\dot{d}\sin q_1\dot{q}_1 - d\cos q_1\dot{q}_1^2 - d\sin q_1\ddot{q}_1 + u_a \\
\ddot{z}_c &= 0.
\end{aligned} \tag{15}$$

According to Assumption 2, the ZMP equations for the simplified model further reduce to:

$$\begin{aligned}
x_{zmp} &= \frac{m_c g x_c - m_c h_c \ddot{x}_c}{(m_0 + m_c)g} \\
y_{zmp} &= \frac{m_c g y_c - m_c h_c \ddot{y}_c - m_0 h_0 u_a - m_c h_c u_a}{(m_0 + m_c)g}.
\end{aligned} \tag{16}$$

It can be seen from (16) that when the linear acceleration of the tracked base is nonzero, only $y_{zmp}$ varies linearly with respect to that acceleration, while $x_{zmp}$ does not change since

$$\left[\frac{\partial x_{zmp}}{\partial u_a}, \frac{\partial y_{zmp}}{\partial u_a}\right]^T = \left[0, \frac{-m_0 h_0 - m_a h_c}{(m_0 + m_c)g}\right]^T. \tag{17}$$

Defining the ZMP "circle" with a variable radius $r$, centered at $(0, -\frac{m_0 h_0 u_a + m_c h_c u_a}{(m_0+m_c)g})$, we can write $r^2 = x_{zmp}^2 + \left(y_{zmp} + \frac{m_0 h_0 u_a + m_c h_c u_a}{(m_0+m_c)g}\right)^2$, so that the center of the "circle" varies linearly with $u_a$, while the radius of the "circle" is independent of $u_a$. Taking the derivative of $r^2$ with respect to time, we get:

$$\frac{dr^2}{dt} = \left(4d^2\dot{q}_1^3\ddot{q}_1 h_c^2 + 4d^2\dot{q}_1\ddot{q}_1 g h_c\right)/g^2. \tag{18}$$

Since $g > 0$ and $h_c > 0$, it immediately follows that $\frac{dr^2}{dt} > 0$ when $\dot{q}_1$ and $\ddot{q}_1$ are of the same sign, and $\frac{dr^2}{dt} < 0$ when $\dot{q}_1$ and $\ddot{q}_1$ are of opposite signs. This demonstrates that the distance from ZMP to the imaginary center $\left(0, -\frac{m_0 h_0 u_a + m_c h_c u_a}{(m_0+m_c)g}\right)$ increases as the magnitude of angular rate $\dot{q}_1$ increases, and vice versa. Thus, according to (17) and (18), the dynamic stability of the feller buncher becomes more compromised as the magnitude of either its linear acceleration or of the first (cabin yaw) joint's acceleration increases.

The result obtained above is based on Assumption 2, and may be rather restrictive in its application. However, in the cases when the assumptions holds, a bang-bang type time optimal control input that ensures dynamic rollover stability can be derived analytically.

## IV. Motion Planning Under Dynamic Stability Constraint

### A. Optimal Control Problem Formulation

In most harvesting scenarios, a common task for a feller buncher is to cut trees, grip them, and place them at a nearby location. The machine itself can be situated on slopes of different grades. With the view to optimizing the efficiency of harvesting operations, the tree manipulation motions should be carried out within the shortest possible time, without the machine rolling over. Naturally, to minimize the overall time required for the feller-buncher to reach final state $\boldsymbol{x}_f$ from an initial state $\boldsymbol{x}_0$ safely, we formulate a constrained nonlinear optimal control problem (OCP) of the form:

$$\begin{aligned}
\min_{\boldsymbol{u}} \quad & \int_{t_0}^{t_f} 1 \ \mathrm{d}t. \\
\text{s.t.} \quad & \dot{\boldsymbol{x}} = g(\boldsymbol{x}, \boldsymbol{u}) \quad \boldsymbol{x}(t_0) = \boldsymbol{x}_0 \quad \boldsymbol{x}(t_f) = \boldsymbol{x}_f \\
& \boldsymbol{p}_{zmp}(\boldsymbol{x}, \boldsymbol{u}) \in Conv(S) \\
& \underline{\boldsymbol{x}} \preccurlyeq \boldsymbol{x} \preccurlyeq \overline{\boldsymbol{x}} \\
& \underline{\boldsymbol{u}} \preccurlyeq \boldsymbol{u} \preccurlyeq \overline{\boldsymbol{u}},
\end{aligned} \tag{19}$$

where $\preccurlyeq$ is defined as vector component-wise inequality, $\underline{\boldsymbol{x}}$ and $\overline{\boldsymbol{x}}$ stand for the lower and upper bounds of the system state $\boldsymbol{x}$, and $\underline{\boldsymbol{u}}$ and $\overline{\boldsymbol{u}}$ stand for the lower and upper bounds of the control input $\boldsymbol{u}$, respectively. The state and input constraints ensure that the machine's configuration, joint rates, and joint accelerations are feasible. The optimal control problem defined in (19) can be solved by using a nonlinear optimal control solver such as GPOPS [26].

### B. Simplified Optimal Control Problem Formulation

*1) Manipulator Planning:* To shorten the computational time so that the motion planner can provide guidance within a reasonable amount of time, the optimal control problem (19) can be reformulated using the equations developed for the simplified model in Section III as:

$$\begin{aligned}
\min_{\tilde{\boldsymbol{u}}} \quad & \int_{t_0}^{t_f} 1 \ \mathrm{d}t. \\
\text{s.t.} \quad & \dot{\tilde{\boldsymbol{x}}} = \tilde{g}(\tilde{\boldsymbol{x}}, \tilde{\boldsymbol{u}}) \quad \tilde{\boldsymbol{x}}(t_0) = \tilde{\boldsymbol{x}}_0 \quad \tilde{\boldsymbol{x}}(t_f) = \tilde{\boldsymbol{x}}_f \\
& \boldsymbol{p}_{zmp}(\tilde{\boldsymbol{x}}, \tilde{\boldsymbol{u}}) \in Conv(S) \\
& \underline{\tilde{\boldsymbol{x}}} \preccurlyeq \tilde{\boldsymbol{x}} \preccurlyeq \overline{\tilde{\boldsymbol{x}}} \\
& \underline{\tilde{\boldsymbol{u}}} \preccurlyeq \tilde{\boldsymbol{u}} \preccurlyeq \overline{\tilde{\boldsymbol{u}}}.
\end{aligned} \tag{20}$$

It is noted that although the number of variables has been reduced, the ZMP constraint employed in (20) is still derived from (5) using information of all joints. Hence, the motions generated by solving the OCP (20) will guarantee rollover avoidance. Also, we point out that in replacing the optimization problem (19) with (20), the dimensionality of the OCP has been reduced from 22 to 4, and the number of control inputs has been reduced from 7 to 2. However, the input constraints can no longer be placed directly on joint accelerations, although in practice, this can be resolved by tightening the bound of $u_d$ until all joint accelerations are feasible.

*2) Mobile Base Acceleration Planning:* Since the configuration space of the simplified model does not include the coordinates of the base, planning of the base motion must be treated separately. Under Assumption 1 only, we know $\ddot{\boldsymbol{p}}_0^{\mathcal{F}_0} = [0, \ddot{y}_0, 0]^T$, and therefore, by taking the partial derivative of $\boldsymbol{x}_{zmp}$ and $\boldsymbol{y}_{zmp}$ with respect to $\ddot{y}_0$, we can see

that $\boldsymbol{x}_{zmp}$ does not change when the base accelerates, and the variation in $\boldsymbol{y}_{zmp}$ can be described by the rate:

$$\frac{\partial \boldsymbol{y}_{zmp}}{\partial \ddot{y}_0} = \frac{-\sum_i m_i z_i}{\sum_i m_i (\ddot{z}_i - g_z)}.$$

For a typical timber manipulation task, it is reasonable to assume that $\ddot{z}_i$'s are negligible and $z_i$'s are constants. Once the optimal control problem is solved using the formulation (20), the margin (as illustrated in Figure 3 for ZMP locus of simplified model) between the upper and lower edges of the support polygon to the planned ZMP trajectory, $d_u$ and $d_l$, respectively, can be found, and an upper and lower bound on the mobile base's linear acceleration can be derived as:

$$d_u \frac{\sum_i m_i g_z}{\sum_i m_i z_i} \leq \ddot{y}_0 \leq -d_l \frac{\sum_i m_i g_z}{\sum_i m_i z_i}. \tag{21}$$

Acceleration of the mobile base can then be planned using the phase plane method [7].

## V. Simulation Results

In order to showcase the importance of ZMP constraints in manipulator motion planning, and the effectiveness of our simplified formulation, the ZMP loci of a feller buncher obtained through MATLAB simulations are presented for two test cases in this section. The machine is modelled after the Tigercat 855E, and can be described with the schematic diagram in Figure 1. The machine is considered to be holding onto a tree, and the machine and the tree's geometric and mass parameters are summarized in Table I. The machine's support polygon is $3.23$ m$\times$ $5$ m rectangle.

The optimal control results in this section are achieved by running the nonlinear optimal control solver GPOPS [26] under MATLAB environment on a Windows desktop with Intel Core i7-4770 3.40 GHz processor. The results have also been verified in the attached video with a feller buncher model created using Vortex physics engine.

### *A. Full Kinematics vs. Simplified Formulation vs. Phase Plane Method*

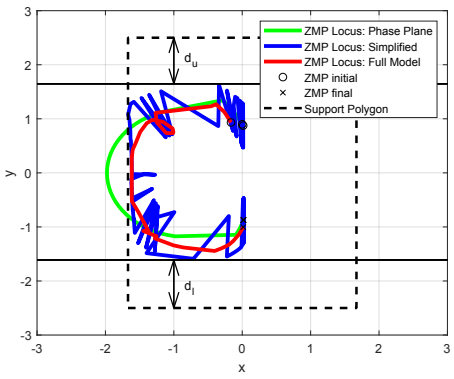


Fig. 3: ZMP loci of constrained motion planning vs. phase plane method.

In the first test case, we consider the feller buncher to be situated statically on a slope that results in a 20-degree roll to the left. The machine starts from an initial condition and the goal is to have the cabin yaw 180 degrees towards left. The ZMP loci of motions generated using the full kinematics optimal motion planning formulation (19), the simplified formulation (20), and the classic phase plane method that considers joint angle, rate, and acceleration limits without stability constraints [7] are presented in Figure 3.

The initial joint angles and velocities are:

$$\begin{aligned} \boldsymbol{q}(t_0) &= [0, -\pi/6, -2\pi/3, \pi/6, -\pi/2]^T \text{ rad} \\ \dot{\boldsymbol{q}}(t_0) &= [0, 0, 0, 0, 0]^T \text{ rad/s}, \end{aligned} \tag{22}$$

and the desired final joint angles and velocities are:

$$\begin{aligned} \boldsymbol{q}(t_f) &= [\pi, -\pi/6, -2\pi/3, \pi/6, -\pi/2]^T \text{ rad} \\ \dot{\boldsymbol{q}}(t_f) &= [0, 0, 0, 0, 0]^T \text{ rad/s}. \end{aligned} \tag{23}$$

The joint rate and acceleration constraints are:

$$\begin{aligned} -\frac{\pi}{4} \leq \dot{q}_i \leq \frac{\pi}{4} \text{ rad/s} \qquad \forall\ i \\ -\frac{\pi}{2} \leq \ddot{q}_i \leq \frac{\pi}{2} \text{ rad/s}^2 \qquad \forall\ i. \end{aligned}$$

The results in Figure 3 show that if the feller buncher follows the time optimal motion prescribed by the phase plane method, the ZMP locus (green) of the machine will travel outside of the support polygon. In this case, the machine is under the risk of rolling over. However, the motion generated through solving (19) and (20) would result in safe (red and blue) ZMP loci. It is noted that although the starting and ending states of the machine for the three motion planning methods are the same, the ZMP loci do not start and end at the same points due to different initial accelerations. The unsafe motion generated by the phase plane method and the safe motions generated by solving the OCP (19) and (20) all take 4.5 seconds to complete.

For the solutions of (19) and (20), the time histories of joint accelerations, rates, and angles are displayed in Figures 4a, 4b, and 4c, respectively. It is noted that all initial and final conditions, and state and input constraints are satisfied for both formulations. However, for this example, the computation time to solve (19) is more than 5 hours, while the computation time to solve (20) is 1.34 seconds.

### *B. Simplified Kinematics Model Optimal Motion Planning with Moving Base*

In the second test case, we consider the feller buncher to be situated on a slope that results in a 15-degree pitch forward and a 15-degree roll to the left. The machine's manipulator arm has to complete the same motion as in the first test case while the mobile base begins at rest, backs up, and goes back to rest during the manipulation. This mobile manipulation task corresponds to a typical occurrence during timber harvesting where the feller buncher has cut a tree on a slope but needs to back up in order to find space to place the tree down. With all joint constraints the same, the mobile base's acceleration has to satisfy $\ddot{y}_0 \in [-2, 2]$ m/s$^2$, and its velocity has to satisfy $\dot{y}_0 \in [-10, 10]$ m/s.

It is after obtaining a solution for the optimal motion of the manipulator, the safe base acceleration bound is found

| Link Number | 0 | 1 | 2 | 3 | 4 | 5 | Tree |
|---|---|---|---|---|---|---|---|
| Length, $l_i$ (m) | 1.60 | 0.96 | 3.27 | 3.27 | 0.458 | 0.677 | 8 |
| Mass, $m_i$ (kg) | 13000 | 5000 | 2000 | 1000 | 50 | 2600 | 4000 |

TABLE I: Machine parameters for the test case.

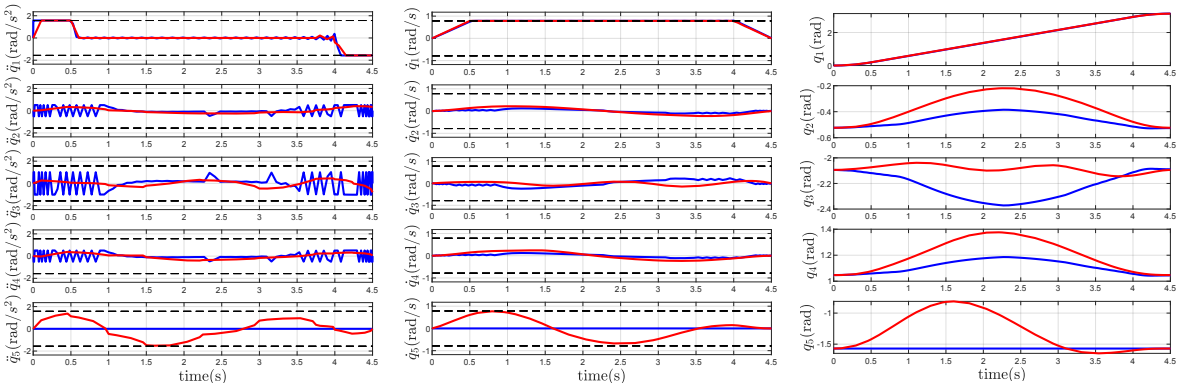


(a) Joint accelerations. (b) Joint velocities. (c) Joint angles.

Fig. 4: Joint accelerations (a), velocities (b), and angle (c) plots. Blue line indicates results from the simplified model, red line indicates results from the full model, and black dashed lines indicate constraints. Note that all of the values related to $q_5$ are zero due to this DoF being reduced in the simplified model.

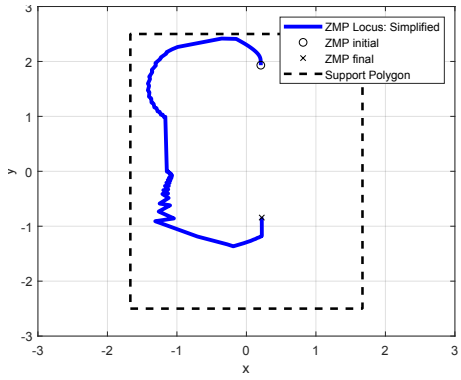


Fig. 5: ZMP locus throughout mobile manipulation task.

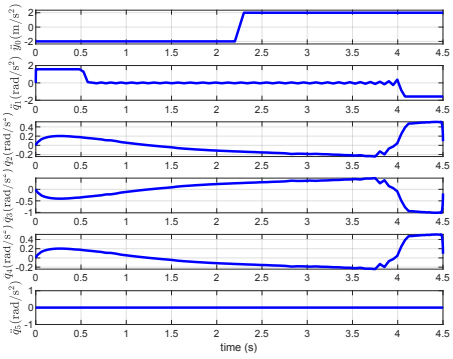


Fig. 6: Base and joint acceleration of the mobile manipulator.

using equation (21). Figure 5 shows that throughout the task, the ZMP locus never exceeds the edges of support polygon. Time history of the mobile manipulator's motion is shown in Figure 6. The manipulation motion takes 4.5 seconds to complete and the computation time for arm manipulation is 1.29 seconds, while the time for calculating the base acceleration bound and base motion planning is negligible since analytical solutions exist.

## VI. Conclusions and Future Work

In this paper, a stability constrained time-optimal motion planning formulation is introduced for a mobile robot. The intended application of the work is for timber manipulation by tree-harvesting machinery. In particular, we consider the feller buncher machine and propose a simplified model for near real-time guidance. With added assumptions, the analytical solution to the problem has also been illustrated. Numerical results obtained for two test cases demonstrate the effectiveness of our proposed method in terms of generating motions that ensure dynamic stability.

The kind of manipulation task our method addresses can also occur in other applications that involve mobile robots operating on rough terrain and manipulating heavy loads, as for example, excavators and mining machinery. To further reduce computation time, the optimization process should be implemented in environments more efficient than MATLAB. Also, methods to address other motions of a feller buncher should be developed to realize the goal of full automation.

## Acknowledgement

This work was supported by the National Sciences and Engineering Research Council (NSERC) Canadian Robotics Network (NCRN), the McGill Engineering Doctoral Awards and Summer Undergraduate Research in Engineering (SURE) programs.

## REFERENCES


[1] O. Lindroos, P. La Hera, and C. Haggstrom. Drivers of advances in mechanized timber harvesting - a selective review of technological innovation. *Croatian Journal for Engineering*, 38(2):243–258, 2017.

[2] E. Papadopoulos and S. Sarkar. The dynamics of an articulated forestry machine and its applications. In *Proceedings of the 1997 IEEE International Conference on Robotics and Automation*, pages 323–328, Albuquerque, New Mexico, April 1997. IEEE.

[3] S. Westerberg, I. R. Manchester, U. Mettin, P. L. Hera, and A. Shiriaev. Virtual environment teleoperation of a hydraulic forestry crane. In *Proceedings of the 2008 IEEE International Conference on Robotics and Automation*, pages 4049–4054, Pasadena, CA, USA, May 2008. IEEE.

[4] P. L. Hera, U. Mettin, S. Westerberg, and A. S. Shiriaev. Modeling and control of hydraulic rotary actuators used in forestry cranes. In *2009 IEEE International Conference on Robotics and Automation*, pages 1315–1320, Kobe, Japan, May 2009. IEEE.

[5] D. O. Morales, S. Westerberg, P. X. La Hera, L. Freidovich, and A. S. Shiriaev. Increasing the level of automation in the forestry logging process with crane trajectory planning and control. *Journal of Field Robotics*, 31(3):343–363, 2014.

[6] D. O. Morales, P. L. Hera, S. Westerberg, L. B. Freidovich, and A. S. Shiriaev. Path-constrained motion analysis: An algorithm to understand human performance on hydraulic manipulators. *IEEE Transactions on Human-Machine Systems*, 45(2):187–199, 2015.

[7] K. G. Shin and N. D. McKay. Minimum-time control of robotic manipulators with geometric path constraints. *IEEE Transactions on Automatic Control*, 30(6):531–541, 1985.

[8] J. E. Bobrow, S. Dubowsky, and J. S. Gibson. Time-optimal control of robotic manipulators along specified paths. *The International Journal of Robotics Research*, 4(3):3–17, 1985.

[9] H. Seraji. A unified approach to motion control of mobile manipulators. *International Journal of Robotics Research*, 17(2):107–118, 1998.

[10] R. Verschueren, N. van Duijkeren, J. Swevers, and M. Diehl. Time-optimal motion planning for n-dof robot manipulators using a path-parametric system reformulation. In *2016 American Control Conference*, Boston, MA, USA, July 2016. IEEE.

[11] H. G. Gibson, K. C. Elliott, and S. P. E. Persson. Side slope stability of articulated-frame logging tractors. *Journal of Terramechanics*, 8(2):65–79, 1971.

[12] E. G. Papadopoulos and D. A. Rey. A new measure of tipover stability margin for mobile manipulators. In *Proceedings of IEEE International Conference on Robotics and Automation*, pages 3111–3116, Minneapolis, MN, USA, April 1996. IEEE.

[13] A. Diaz-Calderon and A. Kelly. On-line stability margin and attitude estimation for dynamic articulating mobile robots. *The International Journal of Robotics Research*, 24(10):845–866, 2005.

[14] M. Mosadeghzad, D. Naderi, and S. Ganjefar. Dynamic modeling and stability optimization of a redundant mobile robot using a genetic algorithm. *Robotica*, 30:505–514, 2012.

[15] N. Bouton, R. Lenain, B. Thuilot, and J. Fauroux. A rollover indicator based on the prediction of the load transfer in presence of sliding: application to an all terrain vehicle. In *Proceedings of the 2007 IEEE International Conference on Robotics and Automation*, pages 1158–1163, Roma, Italy, April 2007. IEEE.

[16] N. Bouton, R. Lenain, B. Thuilot, and P. Martinet. A new device dedicated to autonomous mobile robot dynamic stability: Application to an off-road mobile robot. In *2010 IEEE International Conference on Robotics and Automation*, pages 3813–3818, Anchorage, AK, USA, May 2010. IEEE.

[17] D. Denis, B. Thuilot, and R. Lenain. Online adaptive observer for rollover avoidance of reconfigurable agricultural vehicles. *Computers and Electronics in Agriculture*, 126:32–43, 2016.

[18] M. Vukobratovic and J. Stepanenko. On the stability of anthropomorphic sytems. *Mathematical Biosciences*, 15:1–37, 1972.

[19] S. Sugano, Q. Huang, and I. Kato. Stability criteria in controlling mobile robotic systems. In *Proceedings of the 1993 IEEE/RSJ International Conference on Intelligent Robots and Systems*, pages 832–838, Yokohama, Japan, July 1993. IEEE.

[20] A. Mohammadi, I. Mareels, and D. Oetomo. Model predictive motion control of autonomous forklift vehicles with dynamics balance constraint. In *2016 14th International Conference on Control, Automation, Robotics, and Vision*, pages 1–6, Phuket, Thailand, Nov. 2016. IEEE.

[21] Q. Huang, K. Tanie, and S. Sugano. Coordinated motion planning for a mobile manipulator considering stability and manipulation. *The International Journal of Robotics Research*, 19(8):732–742, 2000.

[22] K. M. E. Dine, J. Corrales-Ramon, Y. Mezouar, and J. Fauroux. A unified mobile manipulator control for online tip-over avoidance based on zmp disturbance observer. In *2018 IEEE International Conference on Robotics and Biomimetics*, pages 1437–1443, Kuala Lumpur, Malaysia, Decemner 2018. IEEE.

[23] J. Kim, W. K. Chung adn Y. Youm, and B. H. Lee. Real-time zmp compensation method using null motion for mobile manipulators. In *2002 IEEE International Conference on Robotics and Automation*, pages 1967–1972, Wangshington, DC, USA, May 2002. IEEE.

[24] D. Choi and J. Oh. Zmp stabilization of rapid mobile manipulator. In *2012 IEEE International Conference on Robotics and Automation*, pages 883–888, Saint Paul, MN, USA, May 2012. IEEE.

[25] S. Lee, M. Leibold, M. Buss, and F. C. Park. Rollover prevention of mobile manipulators using invariance control and recursive analytic zmp gradients. *Advanced Robotics*, 26(11):1317–1341, 2012.

[26] M. A. Patterson and A. V. Rao. Gpops-ii: A matlab software for solving multiple-phase optimal control problems using hp-adaptive gaussian quadrature collocation methods and sparse nonlinear programming. *ACM Transactions on Mathematical Software*, 41(1):1–37, 2014.